The EMBO Journal (2006) 25, 5037–5048 | © 2006 European Molecular Biology Organization | All Rights Reserved 0261-4189/06
www.embojournal.org

THE EMBO JOURNAL

Myelin basic protein-dependent plasma membrane reorganization in the formation of myelin

Dirk Fitzner[1,2], Anja Schneider[1,2], Angelika Kippert[1,2], Wiebke Möbius[2], Katrin I Willig[3], Stefan W Hell[3], Gertrude Bunt[2], Katharina Gaus[4] and Mikael Simons[1,2,*]

[1]Centre for Biochemistry and Molecular Cell Biology, University of Göttingen, Göttingen, Germany, [2]Max-Planck-Institute for Experimental Medicine, Göttingen, Germany, [3]Department of NanoBiophotonics, Max-Planck-Institute for Biophysical Chemistry, Göttingen, Germany and [4]Centre for Vascular Research at the School of Medical Sciences, University of New South Wales, Sydney, NSW, Australia

During vertebrate development, oligodendrocytes wrap their plasma membrane around axons to produce myelin, a specialized membrane highly enriched in galactosylceramide (GalC) and cholesterol. Here, we studied the formation of myelin membrane sheets in a neuron–glia co-culture system. We applied different microscopy techniques to visualize lipid packing and dynamics in the oligodendroglial plasma membrane. We used the fluorescent dye Laurdan to examine the lipid order with two-photon microscopy and observed that neurons induce a dramatic lipid condensation of the oligodendroglial membrane. On a nanoscale resolution, using stimulated emission depletion and fluorescence resonance energy transfer microscopy, we demonstrated a neuronal-dependent clustering of GalC in oligodendrocytes. Most importantly these changes in lipid organization of the oligodendroglial plasma membrane were not observed in shiverer mice that do not express the myelin basic protein. Our data demonstrate that neurons induce the condensation of the myelin-forming bilayer in oligodendrocytes and that MBP is involved in this process of plasma membrane rearrangement. We propose that this mechanism is essential for myelin to perform its insulating function during nerve conduction.

The EMBO Journal (2006) **25,** 5037–5048. doi:10.1038/sj.emboj.7601376; Published online 12 October 2006
Subject Categories: membranes & transport; neuroscience
Keywords: membrane condensation; myelin; myelin basic protein; neurons; oligodendrocytes

Introduction

Oligodendrocytes spirally wrap their plasma membrane around axons to form the myelin membrane sheet during the development of the central nervous system (Pedraza *et al*, 2001; Poliak and Peles, 2003; Sherman and Brophy, 2005). Axonal insulation by myelin not only facilitates rapid nerve conduction but also regulates axonal transport and protects against axonal degeneration (Edgar *et al*, 2004; Yin *et al*, 2006). Myelin is enriched in lipids (70% of total dry weight) and contains a restricted set of proteins, which are primarily found in myelin. The two major central nervous system myelin proteins are the proteolipid proteins (PLP/DM20), highly hydrophobic and cholesterol-interacting proteins with four transmembrane domains, and the myelin basic protein (MBP), a peripheral membrane protein. Studies on the mutant mouse, shiverer, which carries a large deletion of the MBP gene, have demonstrated that MBP is absolutely required for the formation of intact myelin (Roach *et al*, 1985; Readhead *et al*, 1987). The mechanistic function of MBP in the formation of myelin is still not understood. However, the interaction of the highly positively charged MBP to the negatively charged cytoplasmic membrane surface has been suggested to act as a lipid coupler, by bringing the layers of myelin in a close position (Campagnoni and Skoff, 2001; Harauz *et al*, 2004). The insulating properties of myelin might largely be due to its special lipid composition. In contrast to most plasma membranes, myelin contains a high proportion of glycosphingolipids, in particular galactosylceramide (GalC) and its sulfatide derivative sulfate. Both of these two glycosphingolipids are among the most abundant lipids in myelin constituting almost one-third of the lipid mass of myelin. Mice lacking UDP-galactose:ceramide galactosyltransferase, the enzyme required for myelin galactolipid synthesis, compensate this loss by an increased production of the glycosphingolipid, glucosylceramide (Coetzee *et al*, 1996). Glycosphingolipids are of special relevance as they predominantly carry saturated hydrocarbon chains and have a tendency to partition into dynamic lipid domains, called rafts (Brown and London, 2000; Degroote *et al*, 2004; Simons and Vaz, 2004). These domains coalesce after detergent extraction, for example, Triton X-100 or CHAPS into detergent-resistant membranes (DRMs). A more biophysical method to study domain structure is provided by Laurdan (6-dodecanoyl-2-dimethylaminonaphtalene), an environmentally sensitive probe that undergoes a significant spectral shift dependent on the lipid environment. In model membranes, Laurdan's spectral properties can be used to map liquid-ordered and liquid-disordered membrane phases (Bagatolli *et al*, 2003). This dye can also be used in cell membranes to detect raft clusters of condensed membrane as they for examples occur at T lymphocyte activation sites or at the mating tip in yeast cells (Gaus *et al*, 2005; Proszynski *et al*, 2006).

In this work we studied the domain structure of the oligodendroglial membrane and the influence of neurons by combining different microscopy and biochemical approaches. Due to the unique molecular composition of myelin, it serves

*Corresponding author. Centre for Biochemistry and Molecular Cell Biology, Max-Planck Institute for Experimental Medicine, University of Göttingen, Hermann Rein Str. 3, 37073 Göttingen, Germany.
Tel.: +49 551 3899533; Fax: +49 551 3899201;
E-mail: msimons@gwdg.de

Received: 5 May 2006; accepted: 11 September 2006; published online: 12 October 2006

as an ideal model membrane to study the organization of lipid membrane domains in a biological membrane.

Results

Co-localization of myelin membrane components in oligodendrocytes after co-culture with neurons

To study the influence of neurons on the plasma membrane organization of oligodendrocytes, we made use of a co-culture system of oligodendrocytes and neurons in which a rapid and synchronized production of myelin takes place. Co-cultures were prepared by seeding primary oligodendroglial progenitors on differentiated neuronal cultures. By culturing the oligodendrocytes with or without neurons, the influence of the neurons on oligodendrocytes can be directly compared. In both cultures, oligodendrocytes developed an extensive network of branching processes after ~2 days in co-culture. Within the following 3 days, most oligodendrocytes that were cultured without neurons extended large plasma membrane sheets (Figure 1A). In co-culture the majority of oligodendrocytes developed processes that were aligned along neuronal processes (Figure 1A). The formation of myelin in these cultures was demonstrated by electron microscopy (Figure 1B). Oligodendroglial plasma membrane sheets were also observed in co-cultures when oligodendrocytes were seeded onto co-cultures with a lower density of neurons. To characterize the culture system in more detail, we stained cells with antibodies against the major myelin components and compared their distribution after 5 days in culture. In the absence of neurons, PLP was predominantly localized intracellularly and little co-localization with MBP or GalC, which were present in the membrane sheets, was

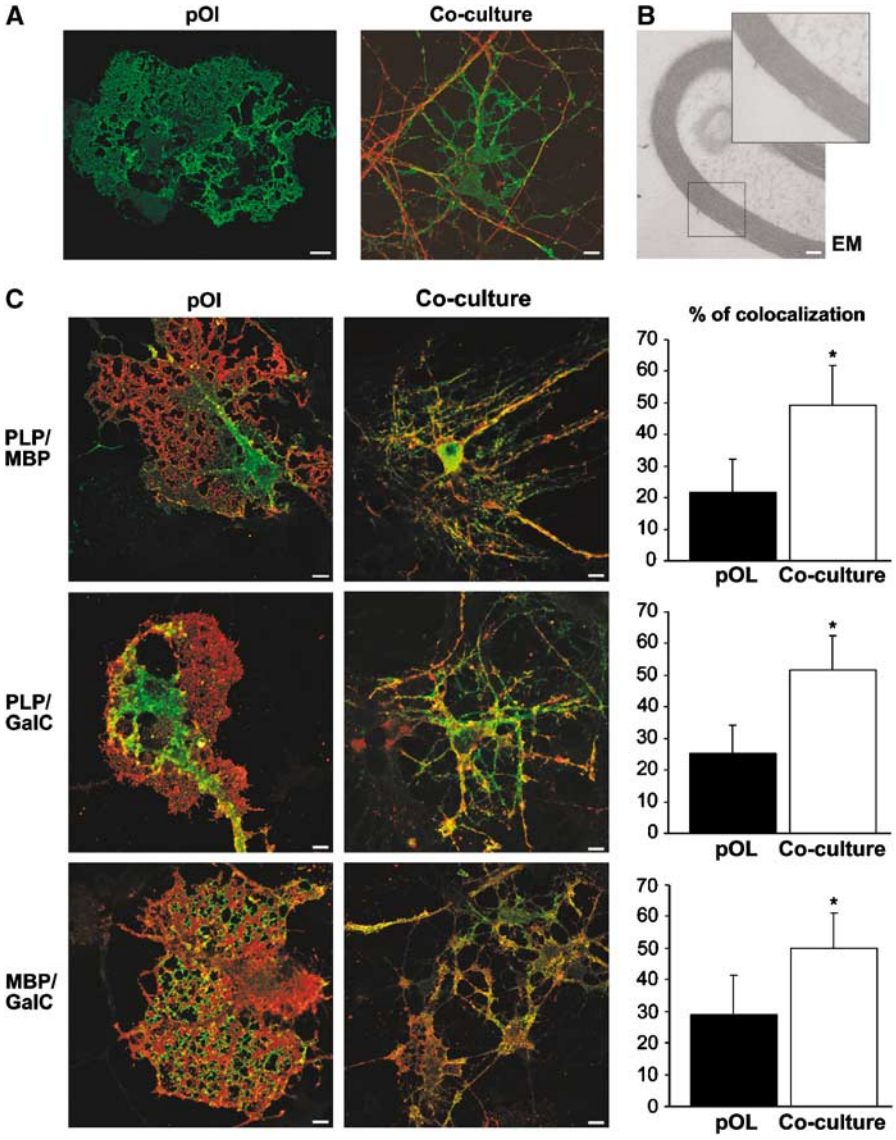

Figure 1 Glia–neuron co-culture system. (**A**) Primary oligodendroglial progenitor cells were seeded on a differentiated neuronal culture (co-culture) or not (pOl), cultured for 5 days, and stained with antibodies against MBP (green) and βIII-tubulin (red) to visualize oligodendrocytes and neurons, respectively. Bar, 10 μm. (**B**) Oligodendrocytes grown for 5 days with neurons form myelin as shown by electron microscopy analysis. Bar, 100 nm. (**C**) Oligodendrocytes grown for 5 days with neurons (co-culture) or not (pOl) were stained for PLP (green), GalC (red) and MBP (red in the upper panel and green in the lower panel). Quantitative analysis of overlap is shown in the graphs ($n = \sim 20$ cells; in %; ±s.d.; *Significantly different from control; $P < 0.001$). Bar, 10 μm.

observed (Figure 1C). In co-culture, co-localization of PLP, MBP and GalC increased substantially (Figure 1C).

Thus, oligodendrocytes cultured without neurons express the major myelin components; however, their subcellular localization as well as the cellular morphology depends on the presence of neurons (Dubois-Dalcq *et al*, 1986; Trajkovic *et al*, 2006).

DRM-association of the oligodendroglial membrane after co-culture with neurons

We used this glia–neuron co-culture system to address the question whether the organization of lipid membrane domains of oligodendrocytes is influenced by neurons. We started our analysis by preparing DRMs, a commonly used biochemical method to analyze the domain organization of membranes (Simons *et al*, 2000; Taylor *et al*, 2002; Schaeren-Wiemers *et al*, 2004). As there are several major caveats to the definition of liquid-ordered membranes as DRMs (Lagerholm *et al*, 2005), we used DRM association only as a possible indicator of changes occurring after co-culture with neurons. To prepare DRMs, oligodendrocytes cultured with or without neurons were extracted with 20 mM CHAPS at 4°C and soluble and insoluble membrane fractions were prepared. We found a higher proportion of PLP and MBP in the CHAPS-insoluble membrane fractions of cells that had been in co-culture with neurons (Figure 2A). This difference was particularly striking for MBP. This was not due to insufficient extraction as the majority of the amyloid precursor protein was soluble in both conditions (Figure 2A). Furthermore, to relate the detergent insolubility of MBP to its association with lipid domains, cultures were subjected to Fumonisin B1 treatment to inhibit sphingolipid biosynthesis. Depletion of sphingolipids reduced the amounts of MBP that could be recovered from the DRM-enriched fraction (Figure 2B). A reduction of GalC levels by Fumonisin B1 treatment was confirmed by TLC (Supplementary Figure S1). DRM association of MBP was also detected in extracts prepared from mice brain and seems to be developmentally regulated, as the fraction gradually increased with the age of the animals (data not shown; DeBruin *et al*, 2005). In agreement, a previous study showed a substantial increase of DRM-associated, myelin-oligodendrocyte glycoprotein in compact myelin as compared to immature, myelin-like membranes of oligodendrocytes in culture (Marta *et al*, 2003). As these results indicated a resistance of myelin to extraction with 20 mM CHAPS at 4°C, we isolated myelin and compared the DRM-associated fraction of lipids. Total myelin lipids and DRM-associated lipids showed similar intensities on TLC plates (Figure 2C). This was in contrast to DRMs prepared from primary cultures of oligodendrocytes, where much less lipids were associated with DRMs (Figure 2C). Together, these results show that the major myelin membrane components can be recovered as a CHAPS-insoluble membrane fraction and suggest an enrichment of liquid-ordered membrane within myelin.

Condensation of the oligodendroglial membrane after co-culture with neurons

As an alternative approach, we used the fluorescent probe Laurdan in conjunction with two photon laser scanning microscopy to visualize the lipid order of the oligodendroglial membrane. Laurdan undergoes a shift in its peak emission

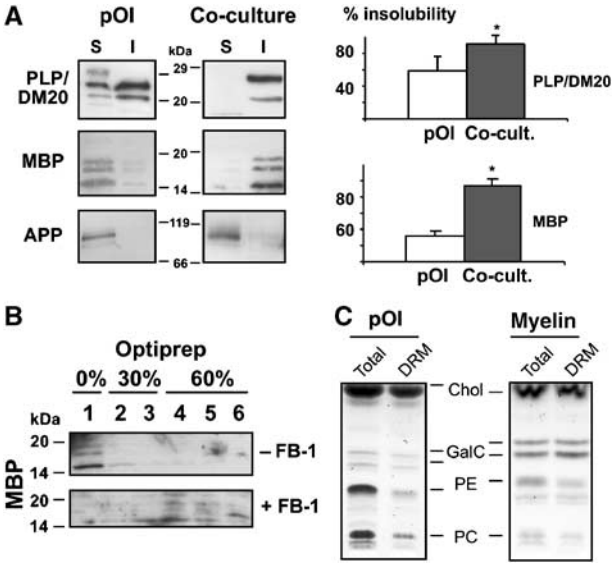

Figure 2 DRM association of oligodendroglial membrane components after co-culture with neurons. (**A**) Primary oligodendrocytes grown for 5 days in the presence (co-culture) or absence of neurons (pOl) were extracted with 20 mM CHAPS for 30 min at 4°C and detergent-insoluble (I) and -soluble (S) fractions were prepared. Quantitative analysis by immunoblotting of 3–5 independent experiments reveals a higher fraction of both MBP (all four isoforms) and PLP (including DM20) within the detergent-insoluble fraction after co-culture with neurons (*Significantly different from control, $P<0.05$). As a control for efficient extraction, the amyloid precursor protein (APP) was detected, as it is not associated with myelin and remains detergent-soluble in both conditions. (**B**) Oligodendrocytes were seeded on neuronal cultures and treated for 3 days with 50 μM of Fumonisin B1 (+FB-1) or left untreated (−FB-1). Cells were extracted with 20 mM CHAPS and subjected to density gradient centrifugation. The top fraction (0% Optiprep) represents the low-density, CHAPS-insoluble membrane fraction, whereas the fractions of higher density contain CHAPS-soluble membranes. (**C**) A lysate of primary oligodendrocytes cultured for 5 days (pOl) or myelin isolated from adult mice was extracted with 20 mM CHAPS in TE buffer or with TE buffer alone, subjected to a density gradient centrifugation, the upper fraction was collected to obtain a DRM or a total membrane fraction (Total), respectively. Analysis by TLC reveals that lipids within myelin are almost completely CHAPS insoluble. The positions of the reference lipids are shown: Chol, cholesterol; GalC, galactosylceramide, PE, phosphatidylethanolamine; PC, phosphatidylcholine.

wavelength from ~500 nm in fluid membranes to ~440 nm in condensed membranes. The fluorescent intensity of Laurdan was recorded simultaneously at both peak emission wavelengths and the normalized ratio representing the generalized polarization (GP) was used to map the lipid order in the cell membranes. Higher GP values stand for a more condensed and ordered membrane—indicative of a raft clustering process. We found that only a small fraction (~16%) of the cell surface of oliogodendrocytes cultured without neurons was covered by areas of high GP values (0.653) (Figure 3A). A similar proportion of liquid-ordered domains have recently been described in the plasma membrane of macrophages (Gaus *et al*, 2003). We also stained oligodendrocytes with an antibody against GalC, a lipid that preferentially associates with liquid-ordered membranes and determined the lipid order of GalC-labelled membrane—for this, GalC confocal images were used to mask the GP images and we obtained a mean GP value of 0.292 ± 0.115 for GalC-positive pixels ($n=43$ images) (Figure 3B). To analyze the influence of neurons on the

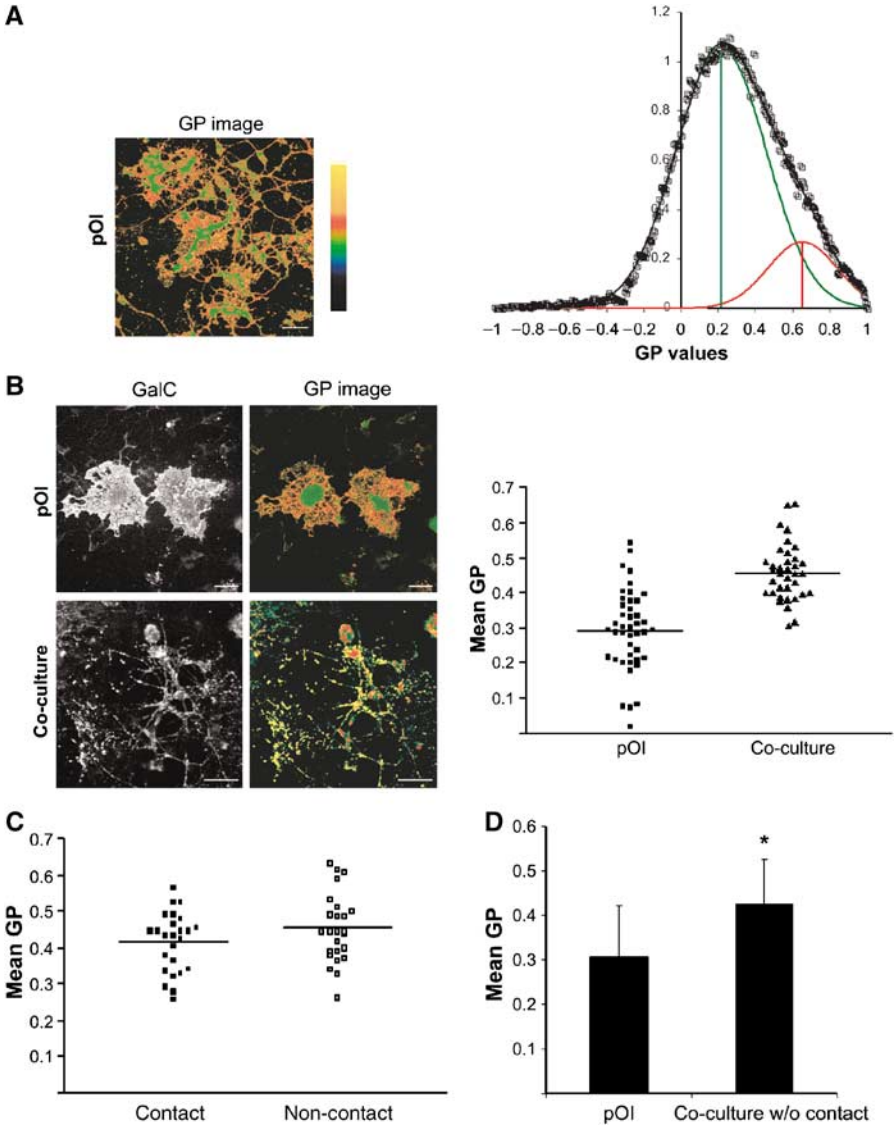

Figure 3 Condensation of the oligodendroglial membrane after co-culture with neurons. (**A**) Laurdan-labelled primary oligodendrocytes cultured without neurons were imaged, intensity images were converted to GP images in pseudo-colour with ordered (GP = 1) to fluid (GP = −1) domains ranging from yellow to green, respectively, as indicated and described in Material and methods. GP distributions ($n > 12$ images) were normalized and fitted to two Gaussian populations (line through data). Green vertical line denotes the center of the fluid populations; red vertical line denotes the center of the ordered populations. (**B**) Oligodendrocytes were grown with (co-culture) or without neurons (pOl), stained with Laurdan, fixed and labelled for GalC. GP values of GalC-positive membranes are presented in the graph ($n > 30$ images). The GP signals shown are masked by the GalC labelling to remove the GP signals from neurons. Horizontal bars indicate the means. Oligodendrocytes in co-culture reveal higher GP values ($P < 0.001$). Bar, 25 μm. (**C**) GP values at the site of cell–cell contacts were determined and compared with the GP values at adjacent non-contact sites ($n = 25$). (**D**) GP values are shown ($n = 35$; *Significantly different from control, $P < 0.001$) for oligodendrocytes cultured for 5 days without neurons or together with neurons but physically separated allowing diffusible, but not contact-mediated factors to act.

glial membrane organization, we repeated the experiments for co-cultures. We observed a dramatic increase in the lipid order of GalC-labelled oligodendroglial membrane (GP value of 0.457 ± 0.081; $n = 36$; $P < 0.001$) (Figure 3B). Because GalC is only found in high levels in oligodendrocytes, the antibody selectively labels oligodendrocytes. These results, obtained with two independent approaches, indicate that neurons induce the condensation of the oligodendroglial membrane.

Next, we analyzed whether the condensation of the membrane is caused by direct cell–cell contact or is initiated by a diffusible factor. First, we compared the GP values at the contact sites with adjacent non-contact sites. We did not observe any substantial differences in membrane condensation at the contact sites with a mean GP value 0.416 ± 0.082 as compared to 0.454 ± 0.094 at non-contact sites ($n = 25$) (Figure 3C). Secondly, we physically separated the neurons from the oligodendrocytes in the co-culture allowing soluble, but not contact-mediated factors to act. When cells were cultured for 5 days without direct contact, we observed a clear increase in membrane condensation (Figure 3D). GP values were 0.308 ± 0.114 in control cells cultured without neurons as compared to 0.426 ± 0.1 ($n = 35$; $P < 0.001$) for cells in co-cultures. These results indicate that membrane condensation is not triggered by direct contact to axons, but instead by unknown soluble factors.

Clustering of GalC in oligodendrocytes depends on neurons

Crosslinking of raft markers leads to the coalescence of small rafts into large clusters (Harder *et al*, 1998). To study this, we labelled GalC in living oligodendrocytes with a primary antibody followed by the subsequent detection by monovalent Fab fragments or bivalent IgG secondary antibodies. The detection with IgG secondary antibodies led to the formation of much larger clusters as compared to the labelling with Fab fragments (Supplementary Figure S2). When the same labelling was performed on oligodendrocytes in co-culture, an intense clustering of GalC was already observed using the Fab fragments and the additional clustering effect of the bivalent secondary antibody occurred; however, it was much less pronounced (Supplementary Figure S2). These results suggest that neurons may induce the clustering of GalC into microscopically visible domains. To analyze this in more detail, we used total internal reflection fluorescence microscopy (TIRFM). TIRFM is based on the excitation with an evanescent wave and allows the selective visualization of fluorophores and thereby cellular processes proximal to the glass-cell surfaces, typically within a range of 70–120 nm. For the TIRFM experiments, we used co-cultures with a lower density of neurons to allow larger areas of the oligodendroglial membrane to contact the glass surface. When living oligodendrocytes were labelled for GalC using monovalent rhodamine-conjugated Fab fragments and were imaged by TIRFM at 37°C, a larger extent of clustering was observed when oligodendrocytes were co-cultured with neurons (Figure 4A and B). We measured the lipid order of the largest

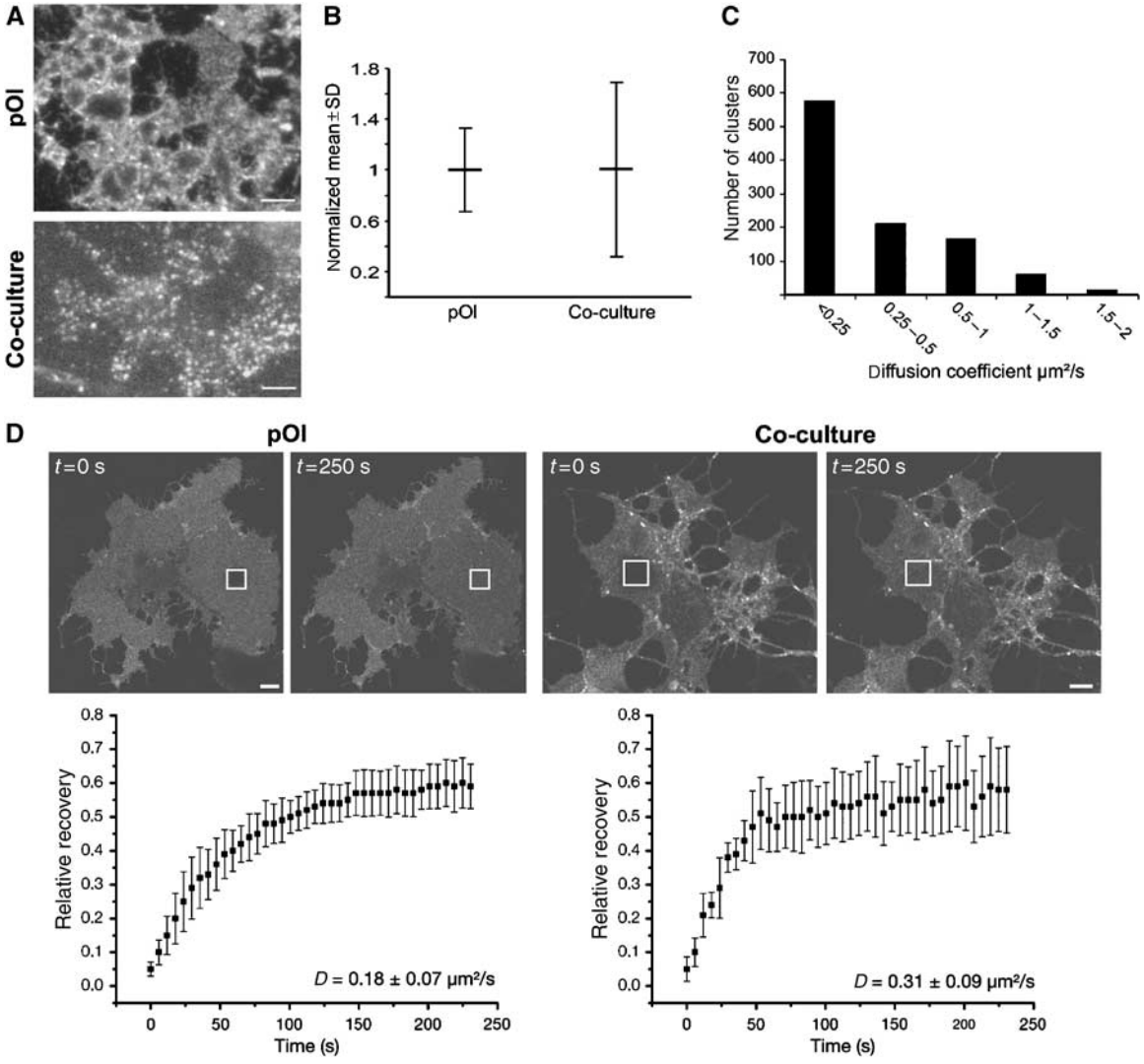

Figure 4 Dynamic GalC-clusters in living oligodendrocytes in culture with neurons. (**A**) Oligodendrocytes grown with (co-culture) or without neurons (pOl) were labelled with a monoclonal antibody against GalC, followed by incubation with rhodamine-conjugated monovalent Fab fragments before imaging with TIRFM at 37°C. (**B**) For quantitative analysis of the degree of clustering, a 750-nm wide line scan was placed within the cells, the fluorescence intensity was recorded, and larger variations of fluorescent intensities were regarded as a higher extent of clustering. The fluorescence intensity signals were normalized to the mean and the variations are expressed as the s.d. of the mean ($n = \sim 5000$ values from 11 cells; see also Supplementary data for more details). Bar, 5 µm. (**C**) Clusters of oligodendrocytes in co-culture were followed by time-lapse TIRFM and the mean-squared displacements (MSD) versus time plots were determined. The resulting diffusion coefficients are shown in the histogram. (**D**) Oligodendrocytes were sequentially labelled with primary antibody against GalC and monovalent rhodamine-conjugated Fab fragments for FRAP measurements. FRAP was measured by bleaching a squared ROI in a flat region of the cell, and fluorescence recovery in these regions was examined. The kinetics of recovery are presented in the graph ($n = 9$; D = diffusion coefficient). Bar, 10 µm.

clusters by Laurdan and found that they have a high GP ratio (0.453 ± 0.116; $n = 25$) indicating highly condensed membrane. By time-lapse TIRFM, we observed that the GalC clusters were mobile, which is also an indication for the viability of the cells and the integrity of the sheets (Figure 4C). Individual clusters revealed multiple modes of diffusions with an average diffusion coefficient of $0.32\,\mu m^2/s$. In some instances, clusters were highly mobile whereas in other cases movement was restricted. This is consistent with previously published modes of diffusion of lipid membrane domains (Schutz *et al*, 2000). Moreover, as an alternative approach to determine the diffusion behavior of GalC-labelled membrane, we applied fluorescent recovery after photobleaching (FRAP). A squared region of interest (ROI) with a width of $\sim 5.5\,\mu m$ was bleached in the membrane sheets of oligodendrocytes grown with or without neurons and the recovery into the bleached area was measured over time. A diffusion coefficient (D) of GalC of $0.31 \pm 0.09\,\mu m^2/s$ for oligodendrocytes in co-culture was measured (Figure 4D). Hence, this population-based measurement is in accordance with the calculations obtained by time-lapse TIRFM. Surprisingly, a lower diffusion coefficient of GalC was observed in oligodendrocytes cultured without neurons ($0.18 \pm 0.07\,\mu m^2/s$). Whether this is due to the changes in the membrane composition or interactions with the cytoskeleton remains to be determined. Taken together, these results indicate that neurons induce the formation of highly dynamic GalC clusters in oligodendrocytes.

To visualize the membrane of oligodendrocytes with a higher resolution, we used stimulated emission depletion (STED), a fluorescence microscopy technique that provides nanoscale optical resolution with a spatial resolution of 60–70 nm in the setup used here (Hell, 2003). With STED microscopy, we observed a higher number of large GalC clusters in oligodendrocytes grown in co-culture as compared to cells cultured without neurons (Figure 5A). The size of these clusters varied within a wide range, having average diameter of ~ 150 nm.

To further analyze the clustering of GalC, we used fluorescence resonance energy transfer (FRET) microscopy. FRET between a donor and acceptor typically occurs in the nanometer range and offers a way of detecting small clusters. For the FRET experiments, we detected GalC in oligodendrocytes with Cy3-(donor) and Cy5-(acceptor) labelled Fab fragments precomplexed with GalC antibodies. The FRET efficiency was measured by donor dequenching upon acceptor photobleaching. FRET measurements revealed that there was very little energy transfer ($E = 0.8 \pm 3.1\%$; $n = 27$) between Cy3- and Cy5-labelled GalC when oligdendrocytes were cultured without neurons (Figure 5C). A marked increase in FRET efficiency ($E = 8.2 \pm 5.3\%$; $n = 48$; $P < 0.001$) was observed upon co-culturing of oligodendrocytes with neurons (Figure 5C). To rule out that this increase in FRET efficiency (E) is a result of an increase in GalC surface density, we plotted E against the acceptor concentration in the ROI (Figure 5D). The surface density of GalC was found to be in a similar range in oligodendrocytes under both culturing conditions and is moreover independent of the acceptor levels (Kenworthy and Edidin, 1998; Varma and Mayor, 1998). Therefore, it can be concluded that the increase in E is not related to changes in acceptor surface density, and may be a result of clustering. As a second criterion for clustering, we analyzed the obtained FRET efficiencies for increasing unquenched donor:acceptor (uD:A) ratios and uD levels (Wallrabe *et al*, 2003). Our analysis revealed that the FRET efficiencies in co-cultures decreased with increasing (uD:A) ratios and uD levels suggesting a clustered distribution of GalC (Figure 5D). Furthermore, we performed FRET experiments with GalC and wheat germ agglutinin, which binds to sialic acid and *N*-acetylglucoaminyl residues, to label the plasma membrane relatively unselectively. We observed a decrease in FRET efficiency between GalC and wheat germ agglutinin after co-culture with neurons (data not shown). Together, these data indicate that the increase in FRET efficiency between different GalC in co-culture is most likely due to a reorganization of the plasma membrane.

MBP is required for oligodendroglial membrane reorganization

Together, these data provide evidence for a raft clustering process. The question arises how this is eventually accomplished. Our finding that neurons induce the surface-localization of the cholesterol-binding protein PLP in oligodendrocytes (Trajkovic *et al*, 2006) led us to investigate a possible role of PLP in the rearrangement of the plasma membrane. We prepared primary cultures from PLP knockout mice and compared those to the corresponding wild-type cultures, but did not detect any differences in the staining pattern of GalC (data not shown). We were also unable to detect any differences in DRM association of MBP in extracts prepared from brains of PLP knockout animals as compared to wild-type animals (data not shown).

Owing to the interaction of MBP with the inner leaflet of the oligodendroglial plasma membrane, MBP was another possible candidate to mediate raft clustering. To test this possibility, we prepared primary cultures from MBP-deleted shiverer mice and compared those to cultures prepared from the wild-type littermates. We used cultures with a low density of neurons to obtain oligodendrocytes with membrane sheets. A higher number of large GalC clusters and a larger degree of clustering were observed within the plasma membrane of wild-type cultures as compared to cultures prepared from shiverer mice (Figure 6A–C). To test whether exogenous expression of MBP could re-establish lipid clustering in oligodendrocytes from shiverer mice, we constructed a recombinant Semliki Forest virus (SFV) encoding the 14 kDa MBP fused to EYFP. We used an MBP-EYFP fusion protein for these experiments to be able to visualize the exogenously expressed protein without the need to permeabilize the plasma membrane as it would change the pattern of GalC staining significantly. To ensure the proper targeting of the fusion protein, we expressed MBP-YFP in co-cultures and confirmed the targeting to myelin (Supplementary Figure S3). When oligodendrocytes from shiverer mice were infected with SFV/MBP-EYFP, the degree of clustering and the number of large GalC clusters increased significantly (Figure 6D). Expression of the EYFP-containing SFV control vector did not cause similar changes.

To obtain further support for a role of MBP in the reorganization of the oligodendroglial membrane, we used Laurdan to visualize the lipid order. Co-cultures were prepared from shiverer and wild-type littermates, labelled with Laurdan and stained for GalC to determine the degree of membrane condensation. Wild-type membranes were highly condensed

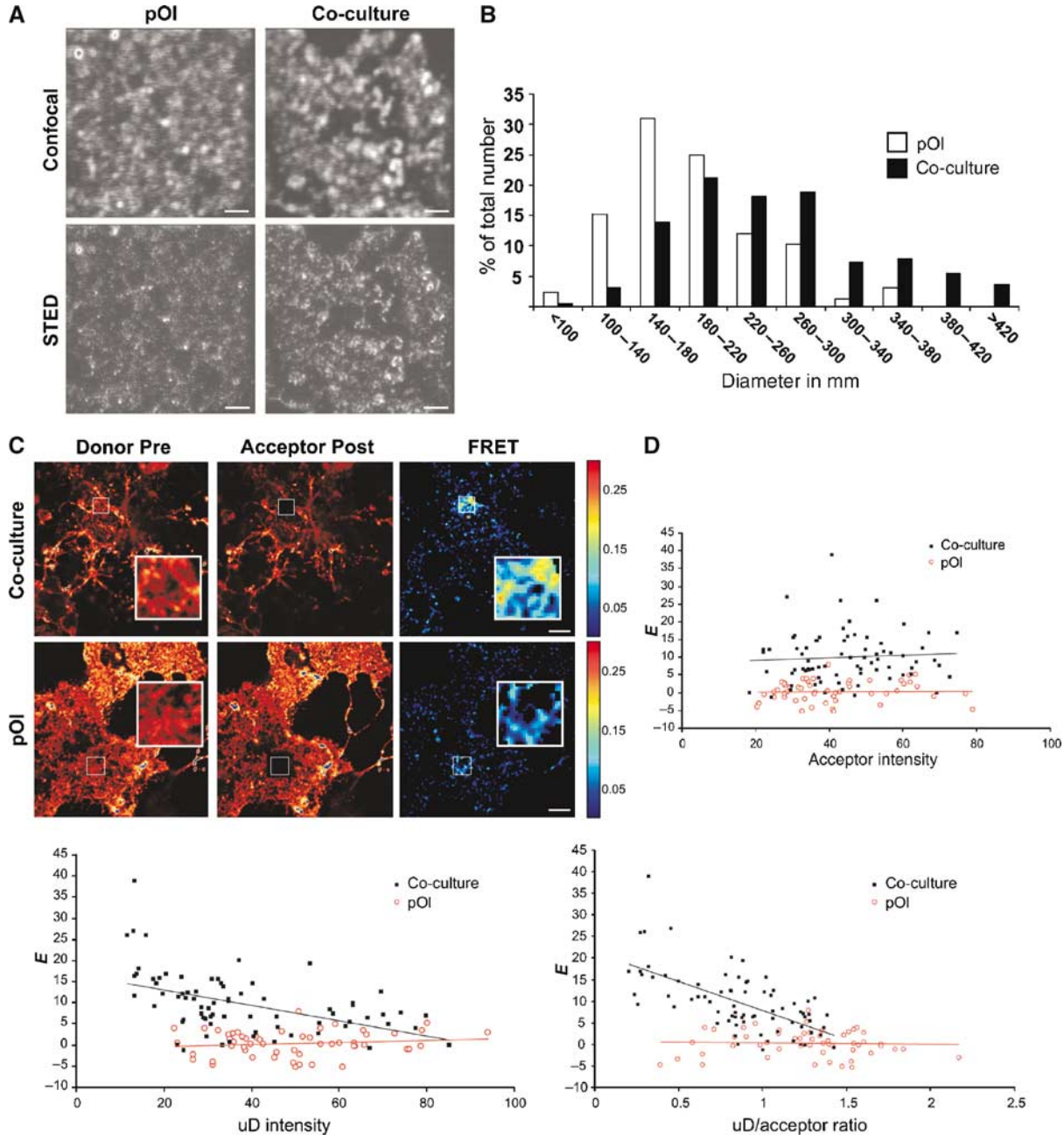

Figure 5 Analysis of GalC clustering by STED and FRET microscopy. Oligodendrocytes were grown with (co-culture) or without neurons (pOl). (**A**) Cells were fixed, sequentially labelled with monoclonal antibodies against GalC and Atto532-conjugated monovalent Fab fragments, and visualized by confocal and STED microscopy. Bar, 1 μm. (**B**) The diameter of clusters in areas of 7.5×7.5 μm was determined and the 15 largest clusters selected for oligodendrocytes grown with or without neurons ($n = 11$ cells). A corresponding histogram of the size distribution of GalC-clusters is shown for oligodendrocytes cultured without (white bar) and with neurons (black bar). (**C**) For FRET measurements, cells were fixed and labelled with a mixture of Cy3- (Donor) and Cy5- (Acceptor) Fab fragments precomplexed with monoclonal antibodies against GalC. Confocal fluorescence images of oligodendrocytes grown with or without neurons are shown before (pre) and after (post) photobleaching of the donor and acceptor, respectively. The acceptor was bleached in the region indicated by the square. The FRET efficiencies [*E*] are represented in an efficiency map in pseudocolor. (**D**) The FRET efficiencies measured for the different ROIs are plotted against the acceptor fluorescence intensities, unquenched donor (uD) levels and uD/acceptor ratios as presented in the graph. Comparison of cells in co-culture with neurons (black squares) reveals higher FRET values than without (red circles), whereas GalC surface densities are in similar ranges. Furthermore, in co-cultures *E* is independent of acceptor levels and decreases with increasing uD levels and uD:A ratios. Bar, 10 μm.

with a mean GP value of 0.450 ± 0.079 ($n = 42$) whereas a marked decrease in the lipid order of GalC-labelled membrane in oligodendrocytes from shiverer mice was observed (0.250 ± 0.073; $n = 30$; $P < 0.001$) (Figure 6E). To further investigate the role of MBP in reorganizing the membrane, we compared DRMs prepared from brain homogenates of shiverer and wild-type mice. PLP was used as a marker to detect possible changes. Whereas the majority of PLP from wild-type mice was CHAPS-insoluble and appeared in the light fraction, a much higher proportion of PLP was found in the heavy fractions in the absence of MBP (Figure 6F). In summary, we conclude that the rearrangement of the oligo-

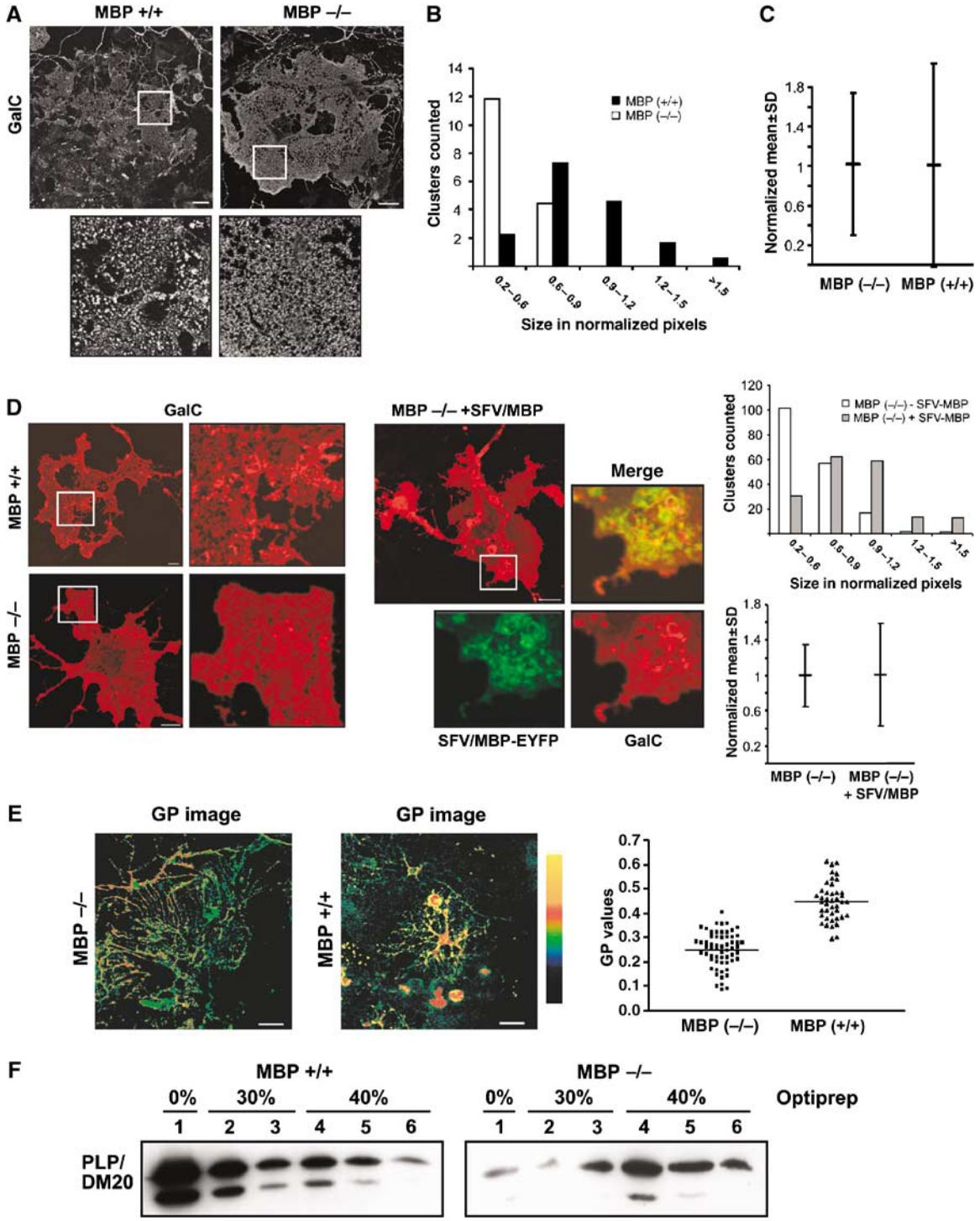

Figure 6 MBP is required for plasma membrane reorganization in oligodendrocytes. (**A**) Primary cultures were prepared from shiverer mice lacking MBP (MBP −/−), and wild-type littermates (MBP + / +). We used cultures with a low density of neurons to obtain oligodendrocytes with membrane sheets. Oligodendrocyts were stained for GalC using the O1 monoclonal IgM antibody. Bar, 20 μm. (**B**) Histogram of the size distribution of GalC-clusters ($n = 150$ clusters) is shown for MBP (−/−) (white bar) and MBP (+ / +) cells (black bar). The sizes are expressed in normalized pixels (see Supplementary data for details). (**C**) The degree of clustering (see Figure 4B and Supplementary data for details) was expressed as the variation in the intensity of the fluorescence singal (normalized mean intensity ± s.d.; $n = \sim 5000$ values from 6 cells). (**D**) Living wild-type (MBP + / +) and shiverer (MBP−/−) oligodendrocytes were surface-stained with a monoclonal IgG antibody against GalC (mAbs GalC) and monovalent Fab fragments. A higher number of large clusters and a higher degree of clustering was found in MBP (+ / +) as compared to (−/−). The expression of MBP-EYFP by the SFV(PD) vector induced the formation of GalC-clusters in MBP (−/−) cells. Histogram of the size distribution of GalC-clusters ($n = 150$ clusters) is shown for MBP (−/−) cells expressing MBP-EYFP (gray bar) or not (white bar). Bar, 10 μm. (**E**) Oligodendrocytes from MBP (−/−) and MBP (+ / +) mice were co-cultured with neurons for 5 days, stained with Laurdan, fixed and labelled for GalC. The GP values are significantly lower in oligodendrocytes from MBP (−/−) mice ($P < 0.001$). Bar, 25 μm. (**F**) Brains from MBP (+ / +) and MBP (−/−) mice were extracted with 20 mM CHAPS and subjected to density gradient centrifugation. Less PLP was recovered from the top fraction (0% Optiprep), the low-density CHAPS-insoluble membrane fraction, in the absence of MBP.

dendroglial plasma membrane upon co-culture with neurons is critically dependent on the presence of MBP.

Discussion

In most biological membranes, rafts are too small and unstable to be directly visualized (Kusumi *et al*, 2004; Lagerholm *et al*, 2005; Hancock, 2006; Marguet *et al*, 2006). Since lipids, in particular cholesterol and the two glycosphingolipids, GalC and its sulfated form, are uniquely enriched in oligodendrocytes; we hypothesized that the organization of lipid domains could be different than in other biological membranes. To study this question, we used oligodendrocytes that were cultured alone or in the presence of neurons to study possible rearrangements of lipid domain organization in the oligodendroglial membrane. Using this model, we detected a considerable increase in raft clustering in the oligodendroglial membrane after co-culture with neurons. Several lines of evidence led us to this conclusion. First, a much larger fraction of myelin membrane components was found in DRMs prepared from co-cultures. Second, Laurdan revealed an increase in the degree of lipid order in the oligodendroglial membrane after co-culture with neurons. Third, evidence for an increase in GalC clustering was observed by TIRF, STED and FRET microscopy when oligodendrocytes were grown in co-culture. Moreover, we provide evidence that this membrane reorganization depends on the function of MBP. Using Laurdan, we found a reduction in the degree of lipid order in oligodendrocytes derived from shiverer mice. In addition, less PLP was associated with DRMs prepared from shiverer brains as compared to DRMs prepared from wild-type mice. Finally, less and smaller GalC-clusters were observed within the plasma membrane of oligodendrocytes from shiverer mice.

It is important to note that a direct visualization of raft domains is technically challenging and most existing methods involve sample preparations that may lead to unintended clustering-induced stabilization of rafts (e.g. fixatives, antibodies, detergents, cold temperature). These technical problems are currently inherent to the field. In our study, the visualization of GalC required the use of antibodies, which may have induced its clustering and therefore changed its native distribution. However, to allow an accurate interpretation we did not rely on one single method, but used a combination of techniques. Most importantly, we base our conclusions on relative data by comparing two conditions. Together, all the different methods used clearly showed an increase in raft clustering in the oligodendroglial membrane after co-culture with neurons.

How is this reorganization of the oligodendroglial membrane achieved? It is possible that the condensation of the membrane occurs by coalescence of pre-existing small and unstable domains. Using Laurdan in conjunction with two-photon microscopy, the detection of areas of condensed membrane is limited to the resolution of the light microscope ($\sim$200 nm). Some small pre-existing GalC-clusters may, therefore, be invisible by this technique. By FRET microscopy, which improves the resolution to a few nanometers, we could only detect significant amount of FRET between individual GalC molecules when oligodendrocytes were cultured in the presence of neurons. Our work is consistent with previous studies suggesting that resting cells contain only (if any) raft domains that are not accessible to microscopic visualization (Munro, 2003; Kusumi *et al*, 2004). For example, recent FRET work on the raft-localized GPI-anchored proteins revealed that only a minor fraction was found in clusters while the majority existed as monomers (Sharma *et al*, 2004). Likewise, single particle tracking of a GPI-anchored protein at a 25-μs resolution only found evidence for small raft assemblies containing few molecules with a lifetime of less than 1 ms (Kusumi *et al*, 2005). In a stimulated state, however, rafts grow in size beyond the optical diffraction limit. In our system, the stimulation occurs by the co-culture of oligodendrocytes with neurons, which leads to the formation of microscopically visible clusters of GalC. Using time-lapse TIRFM, we observed that clusters were mobile and moved within the plane of the oligodendroglial membrane extensions. Coalescence of these mobile assemblies could very well lead to even larger formations, thereby driving the assembly of myelin into a large-scale raft domain. Lipids alone may not be sufficient for such a clustering process. It is likely that proteins mediate the formation and stabilization of condensed membrane domains. Examples of protein mediated raft-clustering are the regulation of immune cell signalling at the immunological synapse or the clustering of raft lipids by GAP43-like proteins (Dykstra *et al*, 2003; Gaus *et al*, 2005). The analogous structural motifs in MBP and MARCKS, a member of the GAP-43 like-family of proteins, are interesting in this aspect (Harauz *et al*, 2000). MARCKS contains a basic domain that binds to acidic phospholipids and this binding of MARCKS to the inner membrane leaflet leads to the formation of large lipid domains that are visible by light microscopy (Laux *et al*, 2000). Our findings with cells from shiverer mice point to a similar function of MBP. Being highly positively charged, MBP may interact with the negatively charged lipids within the inner leaflet side and induce its clustering in analogy to the function of MARCKS. The question of how the binding of lipids in the inner leaflet can lead to a clustering of lipids in the outer leaflet of the lipid bilayer arises. A communication of both leaflets of the bilayer has been demonstrated in previous studies in oligodendrocytes (Dyer and Benjamins, 1988). Antibody-induced clustering of GalC in the outer leaflet led to the formation of large patches of MBP on the inner side of the membrane (Dyer and Benjamins, 1988). Conversely, one can imagine that the binding of MBP to acidic lipids within the inner leaflet may result in clustering of GalC in the outer leaflet of the bilayer. However, the presence of MBP may not be sufficient to induce lipid clustering as the neuronal environment was required for the condensation of the oligodendroglial membrane. One possibility is that neurons regulate a post-translational modification of MBP. An additional explanation is that neurons stimulate the biosynthesis of proteins and/or lipids in oligodendrocytes that can then interact with MBP. In the presence of neurons, MBP may act as a lipid coupler not only bringing the different layers of myelin in close position ('vertical membrane coupling'), but also by clustering the lipid bilayer in lateral dimension ('horizontal membrane coupling'). These mechanisms may be responsible for the concentration of membrane components within myelin and thus the generation and stabilization of large-scale raft domains.

In addition, changes in the lipid composition may result in the growth of the liquid-ordered membrane. Since both

liquid-ordered and disordered membranes are made of different proportions of the same components, changes in lipid synthesis may cause the growth of one domain at the expense of the other. If the changes in the composition occur beyond a critical point, the percolation threshold, a previously discontinuous phase might become continuous (Almeida *et al*, 1993; Meder *et al*, 2006). Myelin may represent a continuous raft-like membrane phase, in which the non-raft membrane is difficult to detect. The presence of liquid-ordered membrane domains over a large area of myelin is contrary to how most other biological membranes are organized. The only other known example is the apical membrane of epithelial cells (Meder *et al*, 2006). The reason may lie in their special function to shield the surrounding area. A less fluid and liquid-ordered membrane may be essential for myelin to fulfil its insulating properties. The biosynthesis of ordered membranes requires a specific mixture of lipids and proteins. This specific mixture of components is even maintained after conditionally knocking out squalen synthetase, an enzyme required for cholesterol biosynthesis in oligodendrocytes (Saher *et al*, 2005). In these mice, oligodendrocytes acquired their cholesterol from an unknown external source, thereby maintaining the stochiometry of myelin components. In comparison, mice lacking UDP-galactose:ceramide galactosyltransferase, the enzyme required for myelin galactolipid synthesis, compensate by an increased production of glucosylceramide (Coetzee *et al*, 1996). Compensation might be so effective, as the production of a highly condensed membrane for which high levels of cholesterol and glycosphingolipids are required is one of the main tasks oligodendrocytes have to accomplish. A key issue to be addressed in the future will be to study how cells adjust the ratio of individual lipids in a membrane. It is intriguing that neurons regulate the plasma membrane levels of PLP in oligodendrocytes by reducing its endocytosis and promoting its exocytosis from late endosomal/lysosomal storage sites (Trajkovic *et al*, 2006). Importantly, a recent analysis has suggested that endocytosis might be one process that limits raft domain size by selective removal of large rafts from the plasma membrane (Turner *et al*, 2005). Regulation of membrane trafficking by neuron to glia signalling may, thus, be one important mechanism of how plasma membrane condensation occurs in oligodendrocytes. As the organization of lipids within the oligodendroglial plasma membrane seems to be regulated by neurons, it will serve as a valuable model system to elucidate the organizing principles of lipid domains in a biological membrane.

Materials and methods

All antibodies used are described in Supplementary data.

Animals and cell culture

The shiverer mutation was maintained on a C57/N backround. The genotype of offsprings was determined by PCR. Primary cultures of oligodendrocytes were prepared from embryonic day 14–16 or postnatal day 1 mice as described (Simons *et al*, 2000). Neurons were selectively removed from the culture by antibody-induced cell lysis after the addition of complement and an antibody directed against neuronal epitope 358 (Trotter and Schachner, 1989). The oligodendroglial progenitors growing on top of a layer of astrocytes were shaken off and cultured further in minimum essential medium, containing B27 supplement, 1% horse serum, L-tyroxine, tri-iodothyroxine, glucose, glutamine, gentamycin, pyruvate and bicarbonate (Sato-B27) on poly-L-lysine-coated dishes or glass-coverslips to obtain a culture enriched in oligodendrocytes.

Myelinating co-cultures were produced by preparing a mixed brain culture from 16-day-old fetal mice. The cells were plated at a density of 50 000–200 000 cells/cm^2 and grown for 2 weeks in Sato-B27. The culture was enriched in neurons, but contained some astrocytes. Primary cultures of oligodendrocytes were seeded on the neuronal culture at a density of 200 000 cells/cm^2. Co-cultures without direct neuron–glia contact were prepared by growing oligodendrocytes and neuronal cultures in the same culture dish but placed on separated glass coverslip facing each other, but separated by a metal ring.

Cloning and production of viral vectors

An MBP-EGFP fusion protein was generated by cloning the 14 kDa MBP cDNA into the pEGFPN1 vector (Clontech) using the *Eco*R1–*Bam*H1 site. The fusion product was subcloned into the *Xho*1–*Not*1 restriction site of the pSFV(PD) vector. In contrast to wild-type SFV vectors, the SFV(PD) expression system is less cytotoxic and therefore allows longer postinfection times (Lundstrom *et al*, 2003). As a control, we used an SFV vector with a fusion protein of EYFP and the N-terminal 13 amino acids of PLP in which the cysteines have been replaced by serines (Schneider *et al*, 2005). Recombinant virus was prepared as described in Supplementary data.

Biochemistry

Detergent extraction was performed as described previously (Simons *et al*, 2002) and as detailed in Supplementary data.

Microscopy and analysis

Immunofluorescence was carried out as described previously (Trajkovic *et al*, 2006). FRAP and FRET experiments were performed and analyzed as described in Supplementary data. Electron microscopy was performed as described previously (Schneider *et al*, 2005). For TIRF imaging a home-built prism-based evanescent field microscope equipped with an Apo L $\times$63 water immersion objective (NA 0.90; Leica) was used (Oheim *et al*, 1998). For live-imaging, coverslips containing the cells were placed in a live cell imaging chamber and observed in imaging medium (HBSS, 10 mM HEPES, 1% horse serum, pH 7.4) at 37°C. Temperature was controlled by a custom-built perfusion system.

For two-photon microscopy, images were obtained with a Biorad microscope. Laurdan (Molecular Probes) labelling was carried out in live cultures (5 μM, 30 min at 37°C), followed by fixation with 4% PFA and immunolabelling. Laurdan was excited at 800 nm with a Verdi/Mira 900 multi-photon laser system (Coherent) and intensities were recorded simultaneously in the range of 400–450 and 470–530 nm for the two channels, respectively. Microscopy calibrations were performed as described previously (Gaus *et al*, 2003).

For STED-microscopy, a home-built setup was used as described in Supplementary data. For data analysis Meta Imaging Series 6.1 software (Universal Imaging Corp.) and ImageJ software (National Institute of Health) were used. All data were acquired with identical camera settings within one experiment. The analysis of microscopy data is described in Supplementary data.

In all experiments statistical differences were determined using the Student's *t*-test. Values are shown as means $\pm$ s.d.

Supplementary data

Supplementary data are available at *The EMBO Journal* Online (http://www.embojournal.org).

Acknowledgements

We are grateful to G Schulz for excellent technical assistance. We thank K-A Nave for discussions and support; J Goncalves, T Lang and J Helenius for help with microscopy analysis; T Campagnoni and K Lundström for reagents; A Esposito and J Goncalves for custom-written Math-lab files. GB is financed by SFB 406. This work was supported by the Deutsche Forschungsgemeinschaft (SFB 523 to MS).

References

Almeida PF, Vaz WL, Thompson TE (1993) Percolation and diffusion in three-component lipid bilayers: effect of cholesterol on an equimolar mixture of two phosphatidylcholines. *Biophys J* **64:** 399–412

Bagatolli LA, Sanchez SA, Hazlett T, Gratton E (2003) Giant vesicles, Laurdan, and two-photon fluorescence microscopy: evidence of lipid lateral separation in bilayers. *Methods Enzymol* **360:** 481–500

Brown DA, London E (2000) Structure and function of sphingolipid- and cholesterol-rich membrane rafts. *J Biol Chem* **275:** 17221–17224

Campagnoni AT, Skoff RP (2001) The pathobiology of myelin mutants reveal novel biological functions of the MBP and PLP genes. *Brain Pathol* **11:** 74–91

Coetzee T, Fujita N, Dupree J, Shi R, Blight A, Suzuki K, Popko B (1996) Myelination in the absence of galactocerebroside and sulfatide: normal structure with abnormal function and regional instability. *Cell* **86:** 209–219

DeBruin LS, Haines JD, Wellhauser LA, Radeva G, Schonmann V, Bienzle D, Harauz G (2005) Developmental partitioning of myelin basic protein into membrane microdomains. *J Neurosci Res* **80:** 211–225

Degroote S, Wolthoorn J, van Meer G (2004) The cell biology of glycosphingolipids. *Semin Cell Dev Biol* **15:** 375–387

Dubois-Dalcq M, Behar T, Hudson L, Lazzarini RA (1986) Emergence of three myelin proteins in oligodendrocytes cultured without neurons. *J Cell Biol* **102:** 384–392

Dyer CA, Benjamins JA (1988) Antibody to galactocerebroside alters organization of oligodendroglial membrane sheets in culture. *J Neurosci* **8:** 4307–4318

Dykstra M, Cherukuri A, Sohn HW, Tzeng SJ, Pierce SK (2003) Location is everything: lipid rafts and immune cell signaling. *Annu Rev Immunol* **21:** 457–481

Edgar JM, McLaughlin M, Yool D, Zhang SC, Fowler JH, Montague P, Barrie JA, McCulloch MC, Duncan ID, Garbern J, Nave KA, Griffiths IR (2004) Oligodendroglial modulation of fast axonal transport in a mouse model of hereditary spastic paraplegia. *J Cell Biol* **166:** 121–131

Gaus K, Chklovskaia E, Fazekas de St Groth B, Jessup W, Harder T (2005) Condensation of the plasma membrane at the site of T lymphocyte activation. *J Cell Biol* **171:** 121–131

Gaus K, Gratton E, Kable EP, Jones AS, Gelissen I, Kritharides L, Jessup W (2003) Visualizing lipid structure and raft domains in living cells with two-photon microscopy. *Proc Natl Acad Sci USA* **100:** 15554–15559

Hancock JF (2006) Lipid rafts: contentious only from simplistic standpoints. *Nat Rev Mol Cell Biol* **7:** 456–462

Harauz G, Ishiyama N, Bates IR (2000) Analogous structural motifs in myelin basic protein and in MARCKS. *Mol Cell Biochem* **209:** 155–163

Harauz G, Ishiyama N, Hill CM, Bates IR, Libich DS, Fares C (2004) Myelin basic protein-diverse conformational states of an intrinsically unstructured protein and its roles in myelin assembly and multiple sclerosis. *Micron* **35:** 503–542

Harder T, Scheiffele P, Verkade P, Simons K (1998) Lipid domain structure of the plasma membrane revealed by patching of membrane components. *J Cell Biol* **141:** 929–942

Hell SW (2003) Toward fluorescence nanoscopy. *Nat Biotechnol* **21:** 1347–1355

Kenworthy AK, Edidin M (1998) Distribution of a glycosylphosphatidylinositol-anchored protein at the apical surface of MDCK cells examined at a resolution of <100 A using imaging fluorescence resonance energy transfer. *J Cell Biol* **142:** 69–84

Kusumi A, Koyama-Honda I, Suzuki K (2004) Molecular dynamics and interactions for creation of stimulation-induced stabilized rafts from small unstable steady-state rafts. *Traffic* **5:** 213–230

Kusumi A, Nakada C, Ritchie K, Murase K, Suzuki K, Murakoshi H, Kasai RS, Kondo J, Fujiwara T (2005) Paradigm shift of the plasma membrane concept from the two-dimensional continuum fluid to the partitioned fluid: high-speed single-molecule tracking of membrane molecules. *Annu Rev Biophys Biomol Struct* **34:** 351–378

Lagerholm BC, Weinreb GE, Jacobson K, Thompson NL (2005) Detecting microdomains in intact cell membranes. *Annu Rev Phys Chem* **56:** 309–336

Laux T, Fukami K, Thelen M, Golub T, Frey D, Caroni P (2000) GAP43, MARCKS, and CAP23 modulate PI(4,5)P(2) at plasmalemmal rafts, and regulate cell cortex actin dynamics through a common mechanism. *J Cell Biol* **149:** 1455–1472

Lundstrom K, Abenavoli A, Malgaroli A, Ehrengruber MU (2003) Novel Semliki Forest virus vectors with reduced cytotoxicity and temperature sensitivity for long-term enhancement of transgene expression. *Mol Ther* **7:** 202–209

Marguet D, Lenne PF, Rigneault H, He HT (2006) Dynamics in the plasma membrane: how to combine fluidity and order. *EMBO J* **25:** 3446–3457

Marta CB, Taylor CM, Coetzee T, Kim T, Winkler S, Bansal R, Pfeiffer SE (2003) Antibody cross-linking of myelin oligodendrocyte glycoprotein leads to its rapid repartitioning into detergent-insoluble fractions, and altered protein phosphorylation and cell morphology. *J Neurosci* **23:** 5461–5471

Meder D, Moreno MJ, Verkade P, Vaz WL, Simons K (2006) Phase coexistence and connectivity in the apical membrane of polarized epithelial cells. *Proc Natl Acad Sci USA* **103:** 329–334

Munro S (2003) Lipid rafts: elusive or illusive? *Cell* **115:** 377–388

Oheim M, Loerke D, Stuhmer W, Chow RH (1998) The last few milliseconds in the life of a secretory granule. Docking, dynamics and fusion visualized by total internal reflection fluorescence microscopy (TIRFM). *Eur Biophys J* **27:** 83–98

Pedraza L, Huang JK, Colman DR (2001) Organizing principles of the axoglial apparatus. *Neuron* **30:** 335–344

Poliak S, Peles E (2003) The local differentiation of myelinated axons at nodes of Ranvier. *Nat Rev Neurosci* **4:** 968–980

Proszynski TJ, Klemm R, Bagnat M, Gaus K, Simons K (2006) Plasma membrane polarization during mating in yeast cells. *J Cell Biol* **173:** 861–866

Readhead C, Popko B, Takahashi N, Shine HD, Saavedra RA, Sidman RL, Hood L (1987) Expression of a myelin basic protein gene in transgenic shiverer mice: correction of the dysmyelinating phenotype. *Cell* **48:** 703–712

Roach A, Takahashi N, Pravtcheva D, Ruddle F, Hood L (1985) Chromosomal mapping of mouse myelin basic protein gene and structure and transcription of the partially deleted gene in shiverer mutant mice. *Cell* **42:** 149–155

Saher G, Brugger B, Lappe-Siefke C, Mobius W, Tozawa R, Wehr MC, Wieland F, Ishibashi S, Nave KA (2005) High cholesterol level is essential for myelin membrane growth. *Nat Neurosci* **8:** 468–475

Schaeren-Wiemers N, Bonnet A, Erb M, Erne B, Bartsch U, Kern F, Mantei N, Sherman D, Suter U (2004) The raft-associated protein MAL is required for maintenance of proper axon–glia interactions in the central nervous system. *J Cell Biol* **166:** 731–742

Schneider A, Lander H, Schulz G, Wolburg H, Nave KA, Schulz JB, Simons M (2005) Palmitoylation is a sorting determinant for transport to the myelin membrane. *J Cell Sci* **118:** 2415–2423

Schutz GJ, Kada G, Pastushenko VP, Schindler H (2000) Properties of lipid microdomains in a muscle cell membrane visualized by single molecule microscopy. *EMBO J* **19:** 892–901

Sharma P, Varma R, Sarasij RC, Ira Gousset K, Krishnamoorthy G, Rao M, Mayor S (2004) Nanoscale organization of multiple GPI-anchored proteins in living cell membranes. *Cell* **116:** 577–589

Sherman DL, Brophy PJ (2005) Mechanisms of axon ensheathment and myelin growth. *Nat Rev Neurosci* **6:** 683–690

Simons K, Vaz WL (2004) Model systems, lipid rafts, and cell membranes. *Annu Rev Biophys Biomol Struct* **33:** 269–295

Simons M, Kramer EM, Macchi P, Rathke-Hartlieb S, Trotter J, Nave KA, Schulz JB (2002) Overexpression of the myelin proteolipid protein leads to accumulation of cholesterol and proteolipid protein in endosomes/lysosomes: implications for Pelizaeus–Merzbacher disease. *J Cell Biol* **157:** 327–336

Simons M, Kramer EM, Thiele C, Stoffel W, Trotter J (2000) Assembly of myelin by association of proteolipid protein with cholesterol- and galactosylceramide-rich membrane domains. *J Cell Biol* **151:** 143–154

Taylor CM, Coetzee T, Pfeiffer SE (2002) Detergent-insoluble glycosphingolipid/cholesterol microdomains of the myelin membrane. *J Neurochem* **81:** 993–1004

Trajkovic K, Dhaunchak AS, Goncalves JT, Wenzel D, Schneider A, Bunt G, Nave KA, Simons M (2006) Neuron to glia signaling triggers myelin membrane exocytosis from endosomal storage sites. *J Cell Biol* **172:** 937–948

Trotter J, Schachner M (1989) Cells positive for the O4 surface antigen isolated by cell sorting are able to differentiate into astrocytes or oligodendrocytes. *Brain Res Dev Brain Res* **46:** 115–122

Turner MS, Sens P, Socci ND (2005) Nonequilibrium raftlike membrane domains under continuous recycling. *Phys Rev Lett* **95:** 168301–168304

Varma R, Mayor S (1998) GPI-anchored proteins are organized in submicron domains at the cell surface. *Nature* **394:** 798–801

Wallrabe H, Elangovan M, Burchard A, Periasamy A, Barroso M (2003) Confocal FRET microscopy to measure clustering of ligand–receptor complexes in endocytic membranes. *Biophys J* **85:** 559–571

Yin X, Baek RC, Kirschner DA, Peterson A, Fujii Y, Nave KA, Macklin WB, Trapp BD (2006) Evolution of a neuroprotective function of central nervous system myelin. *J Cell Biol* **172:** 469–478